

# Lumen Segmentation of Aortic Dissection with Cascaded Convolutional Network

Ziyan Li<sup>1,2,3</sup>, Jianjiang Feng<sup>(✉)1,2,3</sup>, Zishun Feng<sup>1</sup>, Yunqiang An<sup>4</sup>, Yang Gao<sup>4</sup>,  
Bin Lu<sup>4</sup>, and Jie Zhou<sup>1,2,3</sup>

<sup>1</sup> Department of Automation, Tsinghua University, China

<sup>2</sup> State Key of Intelligent Technologies and Systems, Tsinghua University, China

<sup>3</sup> Beijing National Reserch Center for Information Science and Technology, China

<sup>4</sup> Fuwai Hospital, China

**Abstract.** For the diagnosis and treatment of aortic dissection, where blood flows in between the layers of the aortic wall, the segmentation of true and false lumens is necessary. This is a challenging task because the intimal flap separating true and false lumens is thin, discontinuous and has a complex shape. In this paper we formulate lumen segmentation of aortic dissection as the extraction of aortic adventitia (the contour of aorta) and intima (the contour of true lumen). To this end, we propose a cascaded convolutional network for contour extraction on 2-D cross-section images, and then construct a 3-D adventitia and intima shape model. We performed a five-fold cross-validation on 45 aortic dissection CT volumes. The proposed method demonstrated a good performance for both aorta and true lumen segmentation, and the mean Dice similarity coefficient was 0.989 for aorta and 0.925 for true lumen.

**Keywords:** Aortic dissection · Lumen segmentation · Contour extraction · Cascaded convolutional network

## 1 Introduction

Aortic dissection (AD) is a vascular disease with a high mortality rate. Without timely treatment, 1% ~ 2% of the patients with acute type A dissection die in an hour, and nearly half of them die within a week [1]. AD occurs when the aortic intima gets ruptured and detached from the aortic wall, separating aortic lumen into true lumen and false lumen. At present, CT angiography is the standard reference for AD preoperative imaging. The choice of the stent-graft type and size requires accurate quantitative measurements [2]. Therefore, an accurate segmentation of AD CT volumes is important for better visualization and automatic measurement.

However, AD segmentation is a quite challenging task because the intimal flap is a thin membrane structure with an irregular shape, and the intensity distribution inside the lumens varies due to the blood flow variation and the inhomogeneous contrast agent.

---

✉Corresponding author (jfeng@tsinghua.edu.cn).

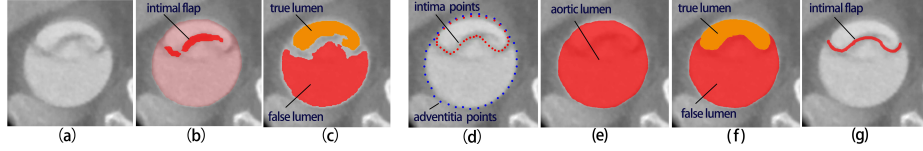


**Fig. 1.** Three different formulations of AD segmentation: (a) original slice, (b) intimal flap segmentation, (c) true and false lumen segmentation, and (d) our proposed adventitia and intima contour extraction. Segmentation results of (b) and (c) require complex post-processing to be converted into each other, while contours in (d) can be easily converted into other representations: (e) aortic lumen, (f) true and false lumens, and (g) intimal flap.

Existing AD segmentation approaches can be categorized into two types based on problem formulation: intimal flap segmentation and lumen segmentation (see Fig. 1). Kovács et al. [3] extracted intimal flaps with a sheetness measure, followed by an extrapolation algorithm to connect the intimal flap with the aortic wall. Krissian et al. [4] presented a comprehensive segmentation of AD by integrating multiple methods (such as level-set algorithm and multiscale vesselness extraction based on gradient and Hessian-matrix), which required manual centerline selection and parameter tuning. Duan et al. [5] extracted intimal flaps by combining Hessian-matrix with spatial continuity between CT slices. However, since Hessian-matrix based methods have little effect on enhancing indistinct intimal flap or blob-like connection point of intimal flap and aortic wall, the intimal flaps obtained from these studies [4, 5] were often not continuous or did not completely separate true lumen from false lumen as illustrated in Fig. 1(b), which require further post-processing.

On the other hand, it is essential to distinguish the true lumen from the false lumen, since the stent-graft should be placed in the true lumen in endovascular treatments [2]. Lee et al. [6] focused on the true-false lumen boundary segmentation by wavelet analysis and generative-discriminative model, without distinguishing the two lumens. Kovács et al. [7] applied an identification method to distinguish between true and false lumens based on a single feature (lumen area) after the segmentation task. Fetnaci et al. [8] segmented true and false lumens separately with a transformed fast marching algorithm. It required a manual seed point to identify the two lumens. These AD segmentation methods, which are based on conventional algorithms, are not robust enough when dealing with blurry intimal flap or noise.

Different from existing approaches, we formulate AD segmentation as the extraction of adventitia and intima contours in order to facilitate quantitative measurement of AD and enable automatic true lumen recognition on cross-sections. In addition, from the adventitia and intima contours we can easily obtain other representations of AD (see Fig. 1). The flowchart of the proposed method is illustrated in Fig. 2.

Inspired by shape regression based on convolutional neural network (CNN) [9], we propose a three-level cascaded convolutional network for a two-step con-

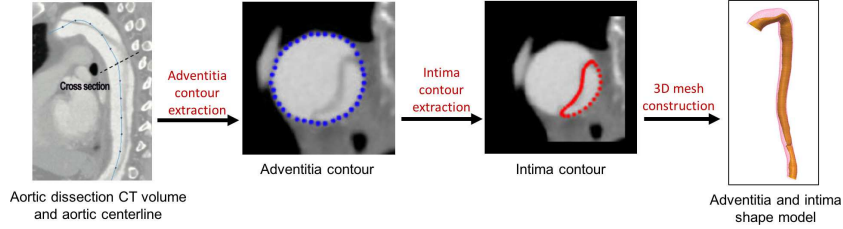


**Fig. 2.** Flowchart of the proposed method

tour extraction. The proposed approach achieved a good performance with the mean Dice similarity coefficient (DSC) reaching 0.989 for aortic lumen and 0.925 for true lumen. From the contours we can easily get the diameters of true and false lumens on different cross-sections, which brings convenience to the quantitative measurement. Another contribution is that, as far as we know, this is the first work where true lumen is distinguished and segmented simultaneously, without manual assistance.

## 2 Methodology

Our proposed method contains three parts (see Fig. 2): First, we intercept cross-sections along the aortic centerlines from CT volumes using the Visualization Toolkit (VTK) (<https://www.vtk.org>), where the centerlines are pre-extracted (see Sect. 3). Then we focus on the two-step contour extraction of adventitia and intima. At last the adventitia and intima shape model is constructed in three-dimension space with VTK.

### 2.1 Contour Model of Adventitia and Intima

True lumen segmentation is meaningful for the treatment of AD, and our main concern is to segment the true lumen by extracting the intima contour. While actually extracting the adventitia contour is much easier, and the intima contour is highly related to the adventitia contour, therefore we build the adventitia and intima model as a whole. In the proposed contour model, the adventitia and intima on each cross-section are represented by a fixed number  $M$  ( $M = 38$ ) of contour points respectively, as illustrated in Fig. 3. Three experienced radiologists helped annotate the cross-section images.

As the adventitia contour always approximates to a circle, we number the adventitia contour points from a fixed starting position counterclockwise at an equal angle interval, so that each point has a certain location on the circle. For aortic intima, if there is no dissection, we index the contour points in the same way as adventitia. Otherwise the contour points of the normal part of intima keep unchanged and the others get detached along with the detached intima (since AD forms because part of the intima gets detached from the aortic wall,

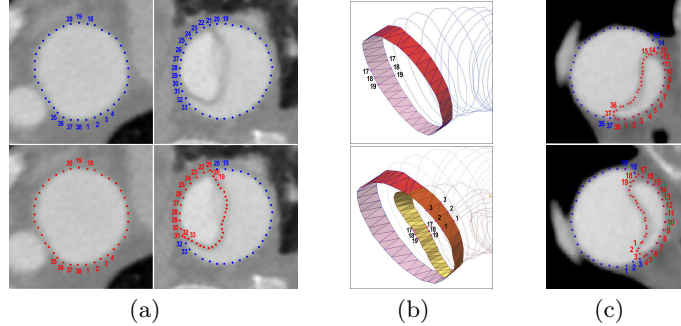


**Fig. 3.** Blue points represent adventitia contour. Red points represent intima contour. (a) First column: a cross-section without dissection, second column: a cross-section with dissection. (b) Connecting method of contour points on adjacent cross-sections (upper: only adventitia, lower: adventitia and intima). (c) Rotation transform.

as introduced in Sect. 1). In this way we can connect two adjacent cross-sections with a triangle-strip by linking the corresponding points and finally construct a regular adventitia and intima shape model (see Fig. 3(b)).

## 2.2 Contour Extraction

Comparing to aortic lumen segmentation, true lumen segmentation is more difficult due to its irregular shape and varying intensity on cross-sections. Some previous works [4, 7] segmented the aorta as ROI before intimal flap segmentation. Inspired by it, we extract the adventitia contour first to guide the intima contour extraction by a scale normalization. For the  $i^{th}$  image  $I_i$  in the dataset, a scale factor  $\lambda_i$  is calculated with its predicted adventitia contour points  $p_{ij}$  ( $p_{ij} \in \mathbb{R}^{2 \times 1}$ ) by:

$$\lambda_i = \frac{r * M}{\sum_{j=1}^M \|p_{ij} - c_i\|_2}, \quad (1)$$

where the image center  $c_i$  is the intersection point of the centerline and  $I_i$ . We set standard radius  $r$  as one-quarter of the image length for a proper foreground size. Then the intima contour point estimation is performed with scaled images.

In the training phase adventitia contour points are initialized by the mean contour of the training set. For intima, we randomly choose a ground-truth from the training set and rescale it as the initial contour. The combinations of different initial contours and training images improve the generalization ability of intima network. In the testing phase both adventitia and intima contour points are initialized by their mean contours of the training set.

To train a robust model, we augment training data on-the-fly by mirror transform, rotation transform and the combination of them. The rotation transform shown in Fig. 3(c) is custom-designed for the contour model. We rotate an image

and its contour points by an angle of  $\theta = t * \theta_0$ , where  $t$  is randomly chosen from  $\{1, 2, \dots, M\}$  and  $\theta_0 = 2\pi/M$ , and then adjust the indexes of contour points in accordance with the contour model in Sect. 2.1. More specifically, the indexes of adventitia points correspond to fixed locations on the circle and will not rotate with the adventitia points, and the indexes of intima points are adjusted according to the indexes of adventitia points as introduced in Sect. 2.1.

**Network Architecture.** The proposed adventitia network and intima network have the same architecture, as shown in Fig. 4. For both adventitia and intima contour points, their positions are associated with the positions of their neighbors. To utilize the coordinate dependences for jointly contour point regression, the first layer takes local patches of contour points as a multi-channel input.

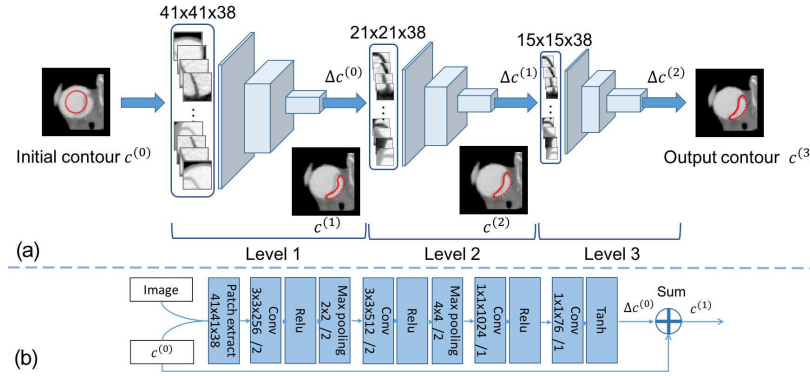


**Fig. 4.** (a) Proposed cascaded convolutional network contains three similar levels. (b) Structure of level 1. (e.g. “Conv  $3 \times 3 \times 256 / 2$ ” means convolutional with  $3 \times 3$  kernels, 256 output features and a stride of 2).

The lumen area and *beak sign*<sup>1</sup> are main visual features to distinguish true and false lumens on cross-sections [10]. To extract these non-local features for rough localization and balance the computation expense, we set the patch size as  $41 \times 41$  pixels in level 1, which is  $21 \times 21$  in level 2 and  $15 \times 15$  in level 3. Three similar cascaded levels with a shrink patch size enable a coarse-to-fine regression of contour points. There are four convolutional layers in level 1 (see Fig. 4(b)), and the last layer with  $1 \times 1$  kernels is followed by *tanh* layer to predict the deviation  $\Delta c^{(0)}$  of the input contour points  $c^{(0)}$  of this level, where  $c^{(0)} = [x_1, y_1, x_2, y_2, \dots, x_M, y_M]^T \in \mathbb{R}^{2M \times 1}$  denotes the coordinates of the contour

<sup>1</sup> The beak sign is an acute angle between the intimal flap and the aortic wall. It only exists in the false lumen.

points. For an image, we define the loss function as:

$$\mathcal{L}(\mathbf{c}^*, \mathbf{c}^{(1)}, \mathbf{c}^{(2)}, \mathbf{c}^{(3)}) = \sum_{i=1}^3 \|\mathbf{c}^{(i)} - \mathbf{c}^*\|_2^2, \quad (2)$$

where  $\mathbf{c}^{(i)}$  denotes the contour predicted by level  $i$ , and  $\mathbf{c}^*$  is the ground-truth. In this way the deviations of contour points of three levels all contribute to the parameter update of our model by back-propagation algorithm.

### 3 Experiments and Results

We collected 45 contrast-enhanced AD CT volumes acquired with a Philips iCT256 scanner at 100 kVp, from 45 different patients with type A dissection (29 patients) or type B dissection (16 patients). The size of volumes is  $512 \times 512 \times Z$  ( $723 \sim 1023$ ) and the voxel spacing is  $X \times X \times 0.8 \text{ mm}^3$  ( $X$  from 0.5507 to 0.7774). To the best of our knowledge, this is the largest evaluation dataset of AD segmentation. The evaluation framework of our lumen segmentation algorithm is similar to [11]. We labeled binary volumes for the dataset with ITK-SNAP (<http://www.itksnap.org>) and then extracted aortic centerlines with VMTK (<http://www.vmtk.org>). There were 4963 cross-section images extracted from the dataset. The pixel spacing of all images was resized to 0.4 mm and the image size is  $144 \times 144$  pixels. In the experiments, we did not consider the starting part of the ascending aorta due to the motion artifact of CT volumes.

Our method was evaluated by a five-fold cross-validation on all 45 cases. The dataset was partitioned into five groups (9 cases per group). We trained the adventitia network first and then the intima network. Network parameters were initialized randomly and learned by SGD with weight decay of 0.0005 and momentum of 0.9. For adventitia network, the learning rate was 0.001 for 8K iterations and then 0.0001 for 2K iterations with the batch size of 256. For intima network, after the same training process as adventitia network, we fine-tuned it with the batch size of 128 and learning rate from  $10^{-4}$  to  $10^{-6}$  (decaying to 1/10 every 4K iterations). The proposed network was built with MatConvNet (<https://github.com/vlfeat/matconvnet>). The training time was 21 hours for adventitia network and 50 hours for intima network, using GTX1080 Ti GPU.

It is hard to make a fair comparison with previous AD segmentation algorithms for the following reasons:

1. The outputs of algorithms are different. The outputs of [4, 5] are intimal flaps.
2. Certain study [8] did not report quantitative result.
3. Study [6] did not consider distinguishing true and false lumens.
4. The datasets used in all these studies are not publicly available.
5. No public implementation is available and a faithful reimplementation is hard.

Hence, we compared our proposed method to the well-known U-net [12], which has achieved high performance in many medical image segmentation tasks

and is publicly available. The U-net was trained to output pixel-wise segmentation results for cross-section images, and for fair comparison, our contour representation is also converted into pixel-wise segmentation. Table 1 reported the segmentation performance of the two methods.

**Table 1.** Evaluation and comparison of lumen segmentation. Mean and relative standard deviation of DSC, sensitivity and specificity are reported.

	Method	DSC	Sensitivity	Specificity
Aortic lumen	U-net	$0.960 \pm 0.026$	$0.958 \pm 0.031$	$0.993 \pm 0.008$
	Proposed	<b><math>0.989 \pm 0.006</math></b>	<b><math>0.990 \pm 0.009</math></b>	<b><math>0.997 \pm 0.003</math></b>
True lumen	U-net	$0.317 \pm 0.808$	$0.356 \pm 0.789$	$0.933 \pm 0.061$
	Proposed	<b><math>0.925 \pm 0.106</math></b>	<b><math>0.921 \pm 0.114</math></b>	<b><math>0.995 \pm 0.008</math></b>

Comparing to manual labeled ground-truth, our method obtained a mean DSC of 0.989 for aortic lumen segmentation and 0.925 for true lumen segmentation. Comparing to the U-net method, the mean DSC of our method was about 3% higher for aortic lumen segmentation. As for true lumen segmentation, we observed that the U-net method was unable to distinguish true lumen from false lumen on cross-sections for pixel-wise segmentation, and therefore resulted in a low DSC, while our method reported a mean DSC of 0.925 with no post-processing.

Fig. 5 shows the extracted contours of some cross-section images. In the cases of bifurcation point and blurry intimal flap, our method can also extract accurate contours. The 3-D adventitia and intima shape models of four cases are presented in Fig. 6. We can see that most parts of AD obtained an accurate segmentation. Only a few positions had poor results, which is mainly because the true and false lumens on cross-sections of these positions had nearly the same shape, area and intensity.

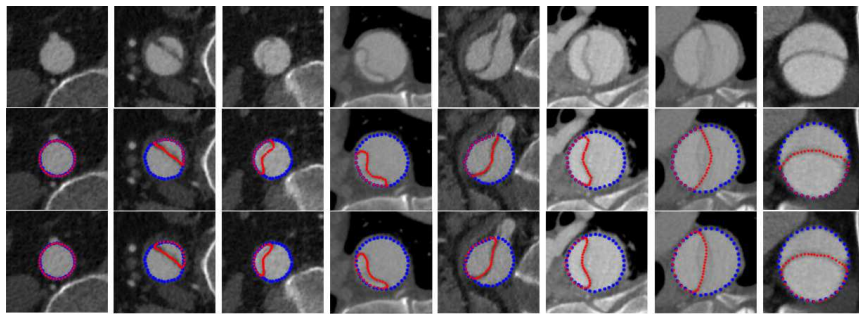


**Fig. 5.** Three rows show the original cross-sections, ground-truth contours and contours extracted by our method, respectively.

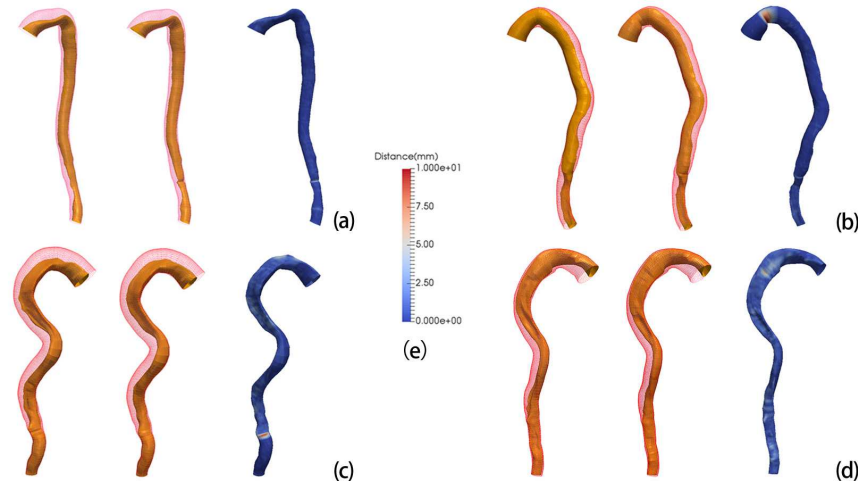


**Fig. 6.** In (a) (b) (c) (d), the adventitia and intima shape models are built by ground-truth (left) and extracted contours (middle), where the inner yellow shape model represents intima and the outer red shape model represents adventitia. The colors of intima shape models (right) represent the distances of intima points between ground-truth and extracted results, with (e) a distance lookup table.

## 4 Conclusion

In this paper, we transform region segmentation of AD into contour extraction by constructing an adventitia and intima shape model, which enables automatic true lumen recognition on cross-sections. Then we present a two-step contour extraction with the proposed cascaded convolutional network. The shape model is built with a fixed number of contour points on each cross-section by a regular connecting method. It suggests their promising applications in quantitative analysis of AD, for instance, measuring diameters of key positions and the volumes of the true and false lumens during follow-ups. Although the closed contour model is beneficial for quantification, AD has locations where the real contour is not closed and may even have complex shape, especially around intima tears. For future work we intend to include these special cases in our model.

**Acknowledgement.** This work is supported by the National Natural Science Foundation of China under Grant 61622207.

## References

1. Nienaber, C.A., Clough, R.E.: Management of acute aortic dissection. *The Lancet* **385**(9970) (2015) 800–811
2. Chiesa, R., Melissano, G., Zangrillo, A., Coselli, J.S.: Thoraco-abdominal aorta: Surgical and anesthetic management. Volume 783. Springer (2011)

3. Kovács, T., Cattin, P., Alkadhi, H., Wildermuth, S., Székely, G.: Automatic segmentation of the aortic dissection membrane from 3D CTA images. In: *International Workshop on Medical Imaging and Virtual Reality*, Springer (2006) 317–324
4. Krissian, K., Carreira, J.M., Esclarin, J., Maynar, M.: Semi-automatic segmentation and detection of aorta dissection wall in MDCT angiography. *Medical Image Analysis* **18**(1) (2014) 83–102
5. Duan, X., Chen, D., Wang, J., Shi, M., Chen, Q., Zhao, H., Zuo, R., Li, X., Wang, Q.: Visual three-dimensional reconstruction of aortic dissection based on medical CT images. *International Journal of Digital Multimedia Broadcasting* **2017**(14) (2017) 1–8
6. Lee, N., Laine, A.F.: True-false lumen segmentation of aortic dissection using multi-scale wavelet analysis and generative-discriminative model matching. *Proceedings of SPIE - The International Society for Optical Engineering* **6915** (2008) 69152V
7. Kovács, T.: Automatic segmentation of the vessel lumen from 3D CTA images of aortic dissection. PhD thesis, ETH Zurich (2010)
8. Fetnaci, N.: 3D segmentation of the true and false lumens on CT aortic dissection images. *Proceedings of SPIE - The International Society for Optical Engineering* **8650**(4) (2013) 86500M
9. Zhang, J., Shan, S., Kan, M., Chen, X.: Coarse-to-fine auto-encoder networks (CFAN) for real-time face alignment. In: *ECCV*, Springer (2014) 1–16
10. LePage, M.A., Quint, L.E., Sonnad, S.S., Deeb, G.M., Williams, D.M.: Aortic dissection: CT features that distinguish true lumen from false lumen. *American Journal of Roentgenology* **177**(1) (2001) 207–211
11. Kirişli, H., Schaap, M., Metz, C., et al.: Standardized evaluation framework for evaluating coronary artery stenosis detection, stenosis quantification and lumen segmentation algorithms in computed tomography angiography. *Medical Image Analysis* **17**(8) (2013) 859–876
12. Ronneberger, O., Fischer, P., Brox, T.: U-net: Convolutional networks for biomedical image segmentation. In: *MICCAI*, Springer (2015) 234–241